Near-Wall Double-Diffusive Convection

Honji, Hiroyuki
Department of Earth System Science and Technology, Interdisciplinary Graduate School of Engineering Sciences, Kyushu University

https://doi.org/10.15017/17254

出版情報：九州大学大学院総合理工学報告. 13 (4), pp.401-408, 1992-03-01. Interdisciplinary Graduate School of Engineering Sciences, Kyushu University

九州大学大学院総合理工学研究科報告
第13巻 第4号 401-408頁 平成4年3月

Engineering Sciences Reports, Kyushu University
(KYUSHU DAIGAKU SOGORIKOGAKU KENKYUKA HOKOKU)
Vol. 13, No. 4, pp. 401 - 408, MAR. 1992

Near-Wall Double-Diffusive Convection

Hiroyuki HONJI*

(Received November 29, 1991)

Double-diffusive convection near a vertical solid wall has been investigated by means of the aluminum-flake method of flow visualization. Two types of fingering flows (normal and large-density-ratio fingers) form near the inside plane surface of the walls of a water tank. Some flow patterns relevant to these two finger regimes are presented.

1. Introduction

Double-diffusive convective flows have been studied extensively in the context of physical oceanography.[1-7] The most intensively investigated one of these is the thermohaline convection. The thermohaline convection may play an important role in the mixing of upper and lower layers of sea water. It has also been suggested that double-diffusive convection has some relevance to geophysical and metallurgical processes.[8] No extensive studies on these processes, however, seem to have been initiated yet.

Apart from these applications, a phenomenon of double-diffusive convection *per se* is of fluid-mechanical interest. In recent years, the so called dissipative structures in diverse flow systems including double-diffusive convection have attracted many investigators.[9-12] Bénard convection which occurs when a layer of fluid is heated from below gives rise to one of the typical dissipative structures (Bénard cells). It was the study of this type of flow that led to evolution of the concept of chaos.[13-16] The double-diffusive convective flows give rise to the dissipative structures more complicated than those due to a single diffusive-component convection.

The purpose of this paper is to report some laboratory results relevant to the double-diffusive (mainly thermohaline) convection occurring near vertical plane walls of a water tank. Many photographs of the convective flow patterns in the tank will be presented.

2. Experimental Apparatus and Procedures

The experiment has been carried out using a 40×30×5 cm water tank made of transparent acrylic resin plates. A side view of the tank is shown in **Fig. 1**, in which a horizontal dotted line indicates the approximate level of the interface between upper (hot salty) and lower (cold fresh) waters in the tank. The depth of the water was kept at about 35 cm, and the top surface of the water was left free during each experimental run.

When thermohaline systems were employed, the experimental procedure was as follows. The tank was first filled with a fresh cold water, in which aluminum flakes were suspended

*Department of Earth System Science and Technology

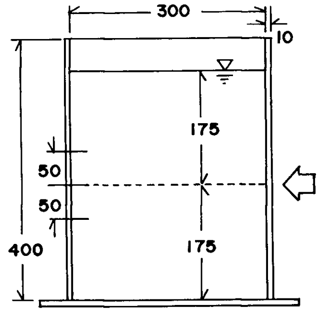

Fig. 1 Water tank (Dimensions in mm): Arrow indicates direction of illumination and 3 levels of thermocouples are shown on the left.

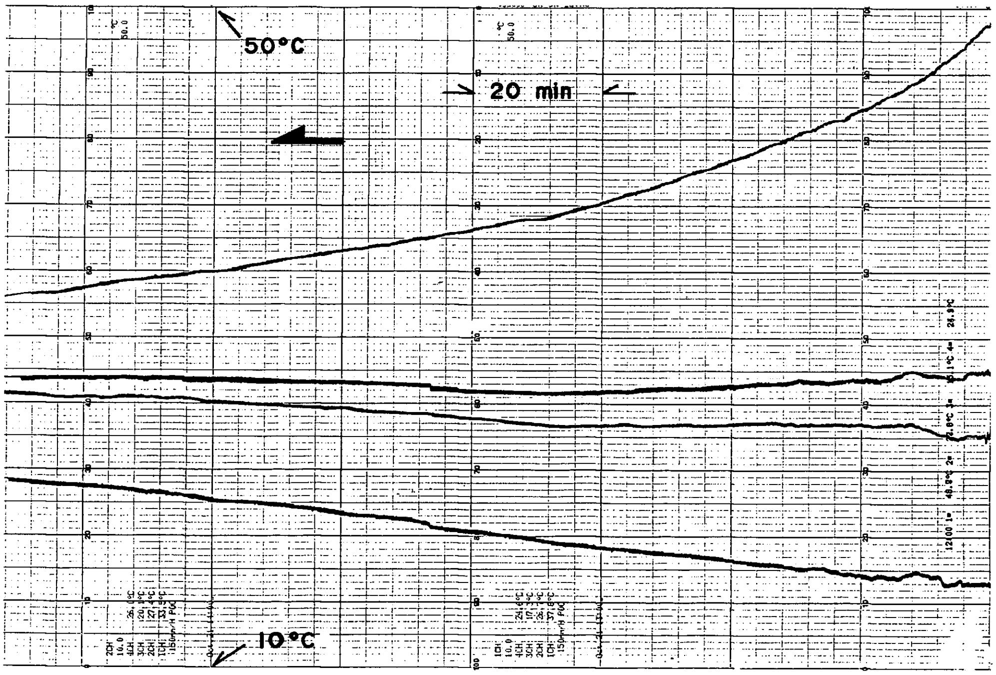

Fig. 2 Water temperature variation during salt finger formation at R=9.5 : Full range of T=40℃.

for visualizing flows. After the water motion came to rest, a piece of a synthetic porous rubber plate was floated softly on the surface of the water. The gap between the rubber plate and the water-tank walls was kept small. Then a hot salty water was poured gently onto the plate out of a watering pot, to fill the upper part of the tank up to the water level of 35cm. The initial salt concentration of upper waters (ΔS) before their pouring into the tank ranged from 0.0033 to 0.67% in weight. The rubber plate was finally removed to have the free top surface, and thereby the experimental setup was completed.

An illumination of the water was made from side using a 1kW slide projector with a narrow slit. The thickness of the illuminated water layer on the inside wall surface was about 0.5cm. In this setup only the lower layer of water was visualized initially. However, as the mixing of the upper and lower waters continued due to salt fingering, aluminum flakes were convected into the upper layer of water to visualize eventually the whole water motions. Visualized flow patterns were photographed from a front side using a 35mm camera.

Measurements of the temperature (T) at 4 different points in the water were carried out by means of a thermocouple data logger. The three positions of thermocouple sensors are shown in **Fig. 1**; another sensor placed at varied positions is not shown here. The resolution of the data logger was 0.1℃. The upper water, lower water, and room temperature ranges were approximately 43-54, 14-23, and 24-26℃, respectively. The difference between initial upper and lower water temperatures (ΔT) before the beginning of convection ranged from 21 to 42℃. A typical time-variation of water temperatures during an experimental run is displayed in **Fig. 2**. The stability density ratio R is here defined as $\alpha \Delta T / \beta \Delta S$, where α and β are the coefficients of thermal expansion and salinity contraction, respectively. The uppermost curve shows the signal from the uppermost thermocouple in a hot salty water. The two curves at the middle show the signals from the sensors near the initial interface level. The lowermost one shows that from the sensor in a cold fresh water. The temperatures approach to a constant value as time increases from right to left in the figure.

3. Results and Discussion

It is well known that salt fingering occurs in thermohaline convection at some appropriate range of parameters.[3] No effects, however, of nearby solid vertical walls on the formation of salt fingers seem to have been investigated in detail. Typical salt finger patterns at an intermediate value of R are shown in **Fig. 3**. An initial stage of fingering near the inside surface of the front wall is displayed in **Fig. 3 (a)**. A dark distorted line in the horizontal direction lies below the mid-height and the fingers are still short. The formation of

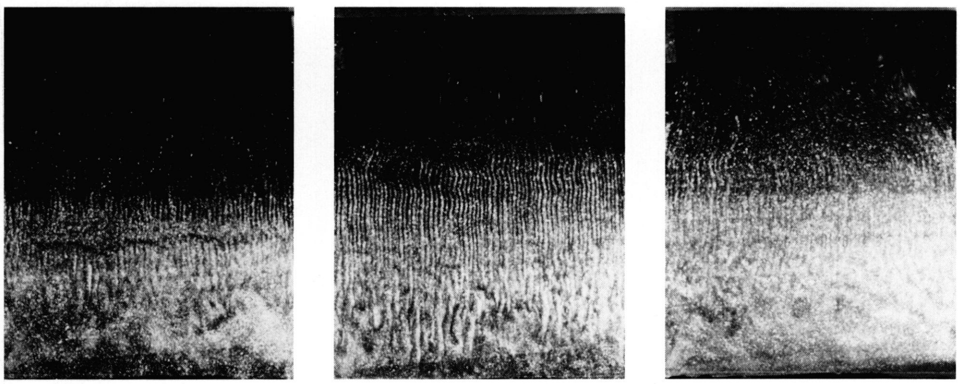

(a) **(b)** **(c)**

Fig. 3 Typical salt fingers (front views) at R=12.

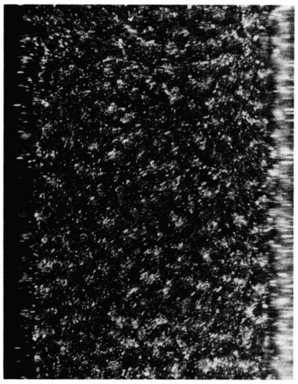

Fig. 4　Cross-sectional view of salt fingers at R=7.3.

the dark line near the wall occurs always when ΔS is relatively small. **Figure 3 (b)** shows a pattern of well-developed salt fingers near the wall, and **Fig. 3 (c)** a pattern of them at the mid-section of the tank. It will be seen that turbulent flows dominate above the fingering region and slow convective flows below that region. Each individual finger is more distinct when it is near the wall as in **Figs. 3 (a)** and **(b)**. A horizontal cross-sectional view of salt fingers seen from top of the tank is also shown in **Fig. 4**, where the flow pattern consists of many finger spots.

The variation of finger patterns near the wall with R is displayed in **Fig. 5** at three different values of R. A typical flow pattern at a lage value of R (corresponding to small ΔS) is shown in **Fig. 5 (a)**. In the figure, horizontally layered waters lie below the initial density interface, and further below them form the short salt fingers with relatively large finger widths. Each finger is quite distinct at the top, but not so at the bottom. The upper part of the tank water remains dark because it is left free from the intrusion of aluminum flakes. **Figure 5 (b)** shows a typical salt finger pattern at an intermediate value of R.

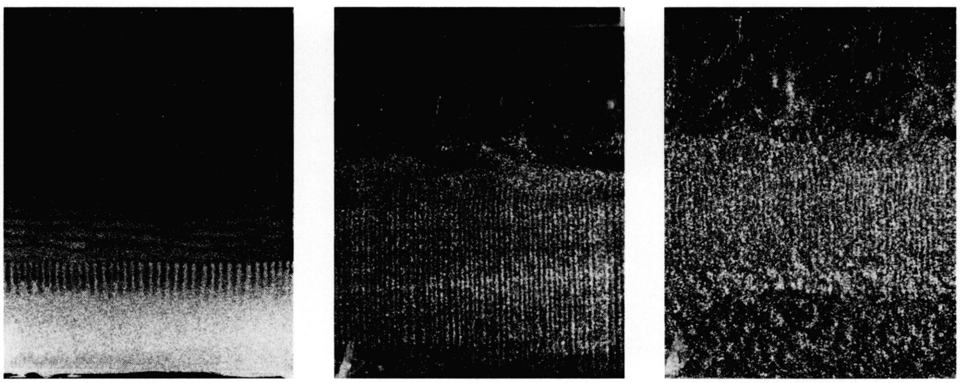

(a)　(b)　(c)

Fig. 5　Variation of salt finger patterns with R.　(a) R=260, (b)=15, (c)=1.4

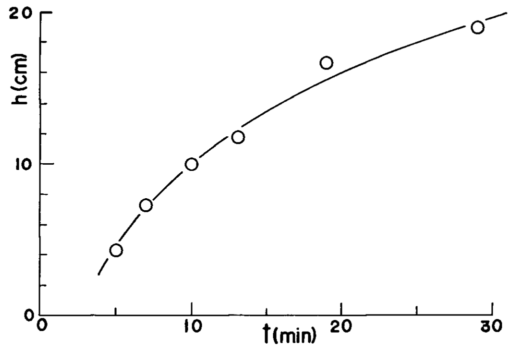

Fig. 6 Development of salt finger length at R=15.

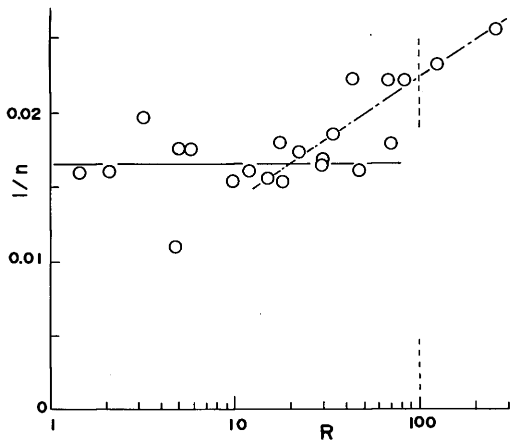

Fig. 7 Dendity stability ratio dependence of mean spacing of salt fingers: A horzontal line indicates normal finger regime and a sloping line large-R finger regime.

The well-developed regularly-spaced fingers are long and distinct. **Figure 5 (c)** shows a finger pattern at a small value of R (corresponding to large ΔS). When R is small, above and below the fingering region appear turbulent convective flows.

The development of near-wall salt fingers in the vertical direction is shown in **Fig. 6**, where h is the vertical length of fingers and t is the time measured from the beginning of convective water motion. The finger length increases monotonically with t. The dependence of the mean horizontal width (1/n) of near-wall salt dingers on R is shown in **Fig. 7**; n is the number of regularly-spaced fingers consisting of an upward moving water column within the tank width of 30 cm. Normal salt fingers have a mean value of $1/n=0.0165$ which gives the mean finger width of about 0.25 cm, and the flow may be called the "normal finger regime". When R is relatively large $(R>20)$, short fingers having large finger widths form in the lower near-wall part of the tank; 1/n for these fingers increases with R. The flow regime at $R>20$ may be called the "large-R finger regime". No fingers have been found to form outside of the range shown in the figure.

The linear stability theory of thermohaline convection is well established.[3] When the thermal and salt Rayleigh numbers are large enough, salt fingers form nearly at $1<R<100$. The above result shown in **Fig. 7** indicates that fingering occured apparently even when $R>100$. Perhaps this is partly due to the fact that the simple use of ΔT for calculating R may not be appropriate because of excessive diffusion near the wall of the tank. Thus the appearance itself of the large-R finger regime shows the near-wall effects on the formation of salt fingers.

When R is extremely large, the flow exhibits a peculiar fingering pattern shown in **Fig. 8**. The flow was first initiated with the formation of a dark horizontal line like the one already shown in **Fig. 3 (a)**. Then upper and lower (near bottom) fingering patterns formed separately. The value of 1/n for the upper fingers are smaller than that for the lower ones. The upper fingers were observed to form over the whole section of the tank, but the lower ones to form only close to the wall. **Figure 9** shows a pattern at the mid-section of the tank for the maximum value of R in the experiment. A peculiar feature of the flow is the formation of a single upward finger, which oscillates left and right very slowly.

Although most of the experiments were concerned with the thermohaline system, a system in which salt is replaced with methanol was tested preliminarily. A fingering pattern for the thermo-alcoholic system is presented in **Fig. 10**. The fingering pattern is similar to the one for the thermohaline system. However, the mean value of 1/n for the thermo-alcoholic fingering patterns has been found to be about 0.0207 cm, which is larger than 0.0165 for the thermohaline fingers. The diffusion coefficients for methanol and salt are of the same order. Because of this, alcoholic detergent often used for washing aluminum flakes to suspend them smoothly in water should be treated with extreme causion. Otherwise there remains a possibility that apparent fingers may not be due to thermohaline convection.

During the formation of fingering patterns the temperatures in convecting waters

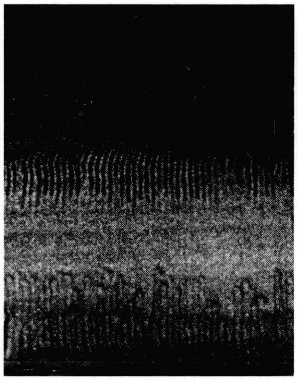

Fig. 8

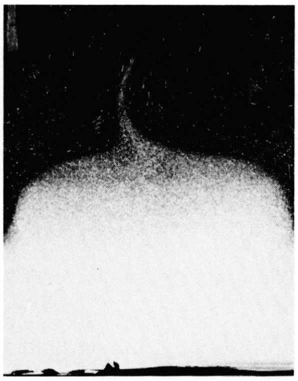

Fig. 9

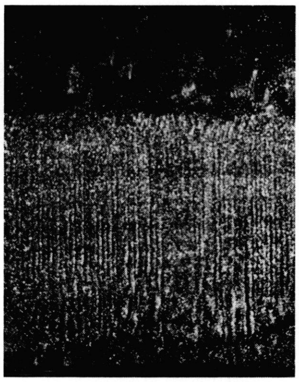

Fig. 10

Fig. 8　Fingering at relatively large R of 44.

Fig. 9　Mid-sectional flow pattern at large R of 370.

Fig. 10　Fingers in thermo-alcoholic system with 1.9% methanol solution.

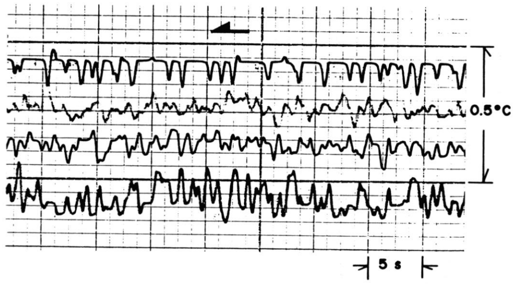

Fig. 11 Temperature fluctuations in salt fingers at R=9.8.

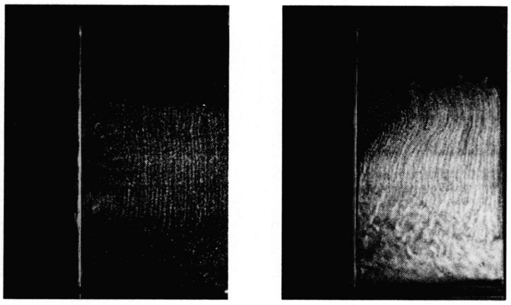

(a) (b)

Fig. 12 Effects of sidewall heating (a) and cooling (b) on fingers.
(a) R=17, (b) 14

exhibit constantly some chaotic fluctuations. An example of time-series data at 4 different points on the level of the initial density interface is shown in **Fig. 11**, in which time increases from right to left. The periods of these fulctuations are very small as compared with the time scale of cooling of the whole double-diffusive system as shown in **Fig. 2**. The small scale fluctuations of upward and downward interchanging water motions themselves may be responsible for these chaotic temperature fluctuations.

The effects of heating and cooling of a sidewall was also investigated by employing an auxiliary smaller 10×40×5 cm tank, which was immersed in a corner of the main tank. When the thermohaline system of water was heated from side, the auxiliary tank was filled with a hot water up to the same level as that of the water in the main tank. When the system was cooled down from side, it was filled similarly with a cold water. Two typical flow patterns are displayed in **Fig. 12**, where **(a)** shows the case of heating and **(b)** the case of cooling. The data of initial water temperatures for **Fig. 12 (a)** are 48.8, 7.5, and 8.1℃ for the upper layer, lower layer, and auxiliary-tank waters, respectively. The corresponding data for **Fig. 12 (b)** are 50.5, 15.9 and 14.3℃, respectively. In the case of sidewall heating (**Fig. 12 (a)**), the salt fingers are disturbed only around the region where the density interface meets the outside vertical side wall of the auxiliary tank. In the case of sidewall cooling (**Fig. 12 (b)**, the initially formed vertical fingers are distorted and pushed rightward around the level of the initial density interface. Both effects are due to the convective flows newly established at the heating or cooling of the sidewall of the auxiliary tank.

In summary, some laboratory results concerning the near-wall double diffusive convection have been presented. Two flow regimes of normal and large-density-ratio fingers have been found to form as well as some peculiar flow patterns at large density ratios. The temperatures in the fingers have also been found to exhibit chaotic fluctuations.

This work was supported by the Grant-In-Aid for Scientific Research (No. 02640294) from the Ministry of Education, Science, and Culture. The author thanks Mrs. Y. Arizumi for her help in the preparation of the manuscript.

References

1) M. E. Stern: Ocean Circulation Physics, Academic Press, N. Y. (1975).
2) A. Masuda: J. Oceanogr. Soc. Jpn., **34**, 8-16 (1978).
3) J. S. Turner: Buoyancy Effects in Fluids, Cambridge University Press, Cambridge (1979).
4) A. J. Williams: J. Geophys. Res., **86**, C3, 1917-1928 (1981).
5) T. Hosoyamada & H. Honji: Rep. Res. Inst. Appl. Mech., Kyushu Univ., **36**, 106, 1-13 (1989).
6) J. Yoshida, H. Nagashima, & H. Niino: J. Geophys Res., **94**, C4, 4923-4937 (1989).
7) J. Yoshida & H. Nagashima: Nagare, **9**, 93-114 (1990).
8) J. S. Turner: Multicomponent Convection, In; Ann. Rev. Fluid Mech., **17**, 11-44 (1985).
9) C. Y. Shen & G. Veronis: Phys. Fluids, **A3**, 1, 58-68 (1991).
10) J. K. Bhattacharjee: Convection and Chaos in Fluids, World Scientific, Singapore (1987).
11) S. Yanase: Nagare, **7**, 1, 3-14 (1988).
12) P. Manneville: Dissipative Structures and Weak Turbulence, Academic Press, London (1990).
13) E. N. Lorenz: J. Atmospheric Sci., **20**, 2, 130-141 (1963).
14) R. Z. Sagdeev, D. A. Usikov, & G. M. Zaslavsky: Nonlinear Physics: From the Pendulum to Turbulence & Chaos, Harwood Academic Publ., Chur (1988).
15) Hao Bai-Lin: Chaos II, World Scientific, Singapore (1990).
16) C. G. Jeevaraj & J. Imberger: J. Fluid Mech. **222**, 565-586 (1991).